Plant Nano Biology 15 (2026) 100226

Contents lists available at ScienceDirect

Plant Nano Biology

journal homepage: www.journals.elsevier.com/plant-nano-biology

Smart delivery of auxin: Lignin nanoparticles promote efficient and safer vascular development in crop species

Rodrigo Faleiro [a,b,*], Marcelo Rodrigo Pace [a], Magda Andréia Tessmer [c], Anderson do Espirito Santo Pereira [d,e], Leonardo Fernandes Fraceto [d], Juliana Lischka Sampaio Mayer [b]

[a] Departamento de Botánica, Instituto de Biología, Universidad Nacional Autómoma de México, Circuito Zona Deportiva s.n., Ciudad Universitaria, Coyoacán, Mexico City 04510, Mexico
[b] Laboratório de Anatomia Vegetal, Departamento de Biologia Vegetal, Instituto de Biologia, Universidade Estadual de Campinas, Campinas, SP 13083-862, Brazil
[c] Laboratório de Pós-Colheita, Departamento de Ciências Biológicas,, Escola Superior de Agricultura "Luiz de Queiroz", Piracicaba, SP 13418-900, Brazil
[d] Universidade Estadual Paulista – Unesp, Instituto de Ciência e Tecnologia de Sorocaba, Departamento de Engenharia Ambiental, Sorocaba, SP 18087-180, Brazil
[e] B. nano Soluções Tecnológicas, Av. Itavuvu, 11.777 - Jardim Santa Cecilia, Sorocaba, SP 18078-005, Brazil

ARTICLE INFO

Keywords:
Nanoencapsulation
Polymeric nanoparticles
Vascular cambium
Vessels
Xylem

ABSTRACT

Xylem is a key tissue responsible for transporting water and nutrients while also providing mechanical support to plants. Its development and function are tightly regulated by plant growth regulators (PGRs), particularly auxins. Recent advances in nanotechnology have introduced promising strategies to modulate plant physiological processes, including the use of nanoparticles that enable controlled PGR release. Among these, lignin nanoparticles (LNPs) are of special interest due to their biodegradability and high encapsulation efficiency. Here, we investigated the effects of foliar application of indole-3-acetic acid (IAA), delivered either in free form and nanoencapsulated within LNPs (LNP–IAA), on xylem tissue development in cherry tomato (a eudicot) and wheat (a monocot). Treatments were applied at 10 and 25 days after sowing, followed by daily qualitative and quantitative assessments of xylem tissue using light microscopy on stem cross-sections. To track the presence of LNPs within vascular tissues, confocal microscopy with fluorochrome-labeled LNPs was employed. Quantitative data were analyzed using generalized linear models (GLMs), correlation analysis, and principal component analysis (PCA). Our results demonstrate that nanoencapsulation preserves and modulates auxin activity, reducing phytotoxic effects observed at higher concentrations. Notably, empty LNPs also elicited biological responses, indicating intrinsic effects of the nanocarrier itself. The responses were species-specific and concentration-dependent, with the highest efficacy observed at 0.05 μg mL^{-1} in cherry tomato and 100 μg mL^{-1} in wheat. Application frequency and plant developmental stage also significantly affected the uptake and utilization of the delivered compound. Importantly, we confirmed the presence of LNPs in stem xylem tissue as early as 1 h after foliar application in both species. Overall, this study highlights the potential of LNPs as sustainable nanocarriers for targeted modulation of vascular development, opening new avenues for xylem bioengineering and growth optimization across divergent plant lineages.

1. Introduction

Xylem is the main tissue responsible for transporting water and minerals along the soil–root–plant continuum, while also providing mechanical support and serving as a storage site (Růžička et al., 2015). Its formation involves distinct developmental pathways. During primary growth, xylem arises from the procambium, giving rise to a vascular axial system composed of conductive elements and associated parenchyma cells. In contrast, during secondary growth — present across lignophytes (including gymnosperms and most angiosperms), with the notable exception of monocots and a few aquatic lineages— the vascular cambium produces both axial and radial systems, ultimately giving rise to wood, one of the most economically valuable plant materials (Evert, 2013). In monocots, which typically lack conventional secondary

* Corresponding author at: Departamento de Botánica, Instituto de Biología, Universidad Nacional Autómoma de México, Circuito Zona Deportiva s.n., Ciudad Universitaria, Coyoacán, Mexico City 04510, Mexico.
E-mail address: rodsfaleiro@gmail.com (R. Faleiro).

https://doi.org/10.1016/j.plana.2025.100226
Received 6 October 2025; Received in revised form 11 November 2025; Accepted 23 November 2025
Available online 26 November 2025

growth, xylem expansion is mediated by alternative thickening meristems, particularly the primary thickening meristem (Pizzolato and Sundberg, 2001). These meristems are highly responsive to biotic stimuli, such as endogenous hormone levels, as well as abiotic factors including growth conditions and environmental variables (Hacke, 2001).

In most eudicotyledons, the establishment and differentiation of the vascular cambium follow the typical lignophyte pattern, characterized by an eustele-type growth (Onyenedum and Pace, 2021). This process begins with the differentiation of the fascicular cambium, followed by the interfascicular cambium, which together form a continuous cambial ring around the stem circumference (Evert, 2013). In contrast, monocots exhibit a distinct organization of vascular bundles within the central cylinder, following a siphonostelic pattern with an atactostelic arrangement (Pizzolato and Sundberg, 2001). In these species, organ growth is primarily driven by the activity of procambium-derived cells and the primary thickening meristem (PTM).

Despite these distinctions, xylem differentiation involves a complex sequence of cellular events, including cell division, differentiation, secondary wall deposition, and, in vessel elements, programmed autolysis (Milhinhos and Miguel, 2013). This process is tightly regulated by the interplay of several plant growth regulators (PGRs), with auxins acting as the main signals that trigger the initiation, division, and differentiation of vascular tissues (Rademacher, 2015). Although auxins participate in numerous processes regulating both vegetative and reproductive development (Paque and Weijers, 2016), their role in vascular meristem signaling is particularly well established in model species. Because xylem represents the bulk of plant biomass and directly influences photosynthetic performance in major crops (thereby affecting grain, fruit, and seed yield) it has become a central target of modern biotechnological research (Růžička et al., 2015).

Nanotechnology is a multidisciplinary field that employs nanoparticles (NPs) and has broad applications across diverse scientific areas, including pharmacology and chemistry (Duhan et al., 2017). In recent years, its use in agriculture has expanded significantly (Athanassiou et al., 2018; Fraceto et al., 2016). By definition, NPs are molecular structures smaller than 100 nm (Auffan et al., 2009). However, more recent studies have suggested extending this threshold to 500 nm, as particles within this range exhibit comparable biological activity (Wang et al., 2022). The advantages of using NPs are mainly attributed to their high surface area and, more importantly, their ability to encapsulate a wide variety of bioactive compounds (Athanassiou et al., 2018). Nanoencapsulation allows sustained release, preventing premature degradation and thereby enhancing compound stability and effectiveness (do Espirito Santo Pereira et al., 2021). Because of their targeted delivery and increased efficiency, nanoformulations can achieve equal or superior biological effects at much lower concentrations compared to conventional treatments.

In agricultural applications, the size and surface charge of nanoparticles (NPs) are critical determinants that directly influence their behavior, absorption, and transport within plants (Zhang et al., 2023). For foliar applications, stomata serve as the main entry points, whereas in soil-based treatments, lateral and adventitious roots fulfill this same role (Avellan et al., 2021). These physicochemical characteristics are essential for optimizing NP performance, as they govern biological interactions and movement through plant tissues. NP concentration also plays a pivotal role in shaping plant responses: most studies report beneficial effects at low concentrations but note oxidative stress and phytotoxicity at higher doses, regardless of NP composition. Nanoparticles are generally divided into two main categories: inorganic NPs, typically composed of metallic elements such as silver (NDABA et al., 2022; Quintela et al., 2024; Yan and Chen, 2019), and polymeric NPs, usually derived from biological polymers such as chitosan (Korpayev et al., 2021; Maruyama et al., 2016; Pereira et al., 2017).

Polymeric nanoparticles have gained increasing attention in agriculture due to their biodegradable nature, making them particularly suitable for sustainable crop production (Campos et al., 2022). Numerous studies have demonstrated their effectiveness in enhancing seed germination, plant growth, and overall crop yield, including both fruit and seed production, across a wide range of species (Faleiro et al., 2025; Pereira et al., 2019; Preisler et al., 2022). Among these formulations, lignin nanoparticles (LNPs) stand out for their multifunctional advantages, such as antifungal activity, UV protection, and cost-effective production with minimal chemical input (Chauhan, 2020; Low et al., 2021; Pereira et al., 2022). LNPs have proven effective both when applied alone (Del Buono et al., 2021) and as carriers encapsulating plant growth regulators (PGRs) such as auxins (Faleiro et al., 2025) and gibberellins (Falsini et al., 2019).

In our previous research with cherry tomato plants, we observed that auxin encapsulated in lignin nanoparticles (LNP–IAA) induced concentration-dependent changes in xylem development by the end of the production cycle (Faleiro et al., 2025). However, the specific mechanisms through which LNP–IAA influences xylem differentiation remain poorly understood. Although the role of exogenous auxin in promoting xylem formation is well established, most studies have focused on model species (Bhalerao and Fischer, 2017; Johnsson et al., 2019; Růžička et al., 2015), leaving a significant gap in knowledge regarding economically important crops. More critically, no study has systematically compared the effects of plant growth regulators (PGRs), either in free or nanoencapsulated form, on meristematic activity and xylem development (both primary and secondary) across major plant lineages, such as eudicots and monocots. Addressing this gap represents a key frontier in elucidating how divergent plant lineages differentially respond to biochemical and nanotechnological modulation of vascular development.

Building on recent evidence demonstrating the effectiveness of lignin nanoparticles (LNPs) and the limited knowledge regarding their effects on vascular tissues, this study presents a temporal and anatomical evaluation of xylem development in the stems of cherry tomato and wheat following foliar application of indole-3-acetic acid (IAA). We assessed vascular responses after two application events, examining how concentration and formulation (free IAA vs. LNP-encapsulated IAA) influence xylem growth dynamics in species with contrasting vascular architectures. Confocal microscopy was further employed to trace LNP localization within stem tissues. Specifically, this study aimed to (1) establish a timeline for IAA-induced xylem modifications and (2) compare the efficacy of nanoencapsulation relative to the free hormone. The results provide foundational insights for optimizing nanocarrier systems in crop improvement. Overall, our findings contribute to a deeper understanding of plant growth regulator delivery mechanisms and support sustainable strategies to enhance plant growth and vascular development.

2. Material and methods

2.1. Materials

For this study, we selected seeds of *Solanum lycopersicum* cv. ‘Sweet Grape’ (cherry tomato), and *Triticum aestivum* (wheat). These species were chosen due to their significant economic impact on agriculture and their distinctive patterns of xylem tissue development. The lignin was purchased from Sigma Aldrich, in which the mainly source is from wood pulp, primarily pine.

2.2. Preparation and characterization of LNP, LNP-IAA, and LNP-labeled

The NPLs were synthesized follow a modified version of the anti-solvent method described by Falsini et al.(2019). The organic phase was prepared by dissolving 6 mL of lignin (5 mg/mL) in a 70 % ethanol solution under magnetic stirring. To this solution, 0.105 mg of carvacrol and 2 mg of IAA (Sigma-Aldrich, Brazil) were added, and the mixture was stirred until fully dissolved. Subsequently, the lignin solution was

poured into 30 mL of water and stirred for 30 min. Afterward, ethanol was removed via rotary evaporation, and the final volume was adjusted to 20 mL. For fluorescent labeling, 0.1 % (relative to lignin mass) of the fluorophore 1,2-dipalmitoyl-sn-glycero-3-phosphoethanolamine-N-(-Lissamine rhodamine B sulfonyl chloride) was incorporated into the organic phase.

The size distribution and polydispersity index of the nanoparticles were determined using the Dynamic Light Scattering (DLS) technique, with scattered light detected at a 90° angle using a Zetasizer Nano ZS90 instrument (Malvern Instruments, UK). Zeta potential was measured using the same instrument via the electrophoresis method. All samples were analyzed in triplicate at 25 °C. The encapsulation efficiency and quantification of the active ingredient (IAA) were analyzed using the HPLC technique. For the release profile of IAA, in vitro release kinetics were evaluated using a two-compartment dialysis system, following the same methodology described in Faleiro et al. (2025).

2.3. Treatments

To evaluate the efficiency of lignin nanoparticles encapsulating auxin, the following treatments were applied: distilled water (control), lignin nanoparticles (LNPs) [100 μg/mL], lignin nanoparticles with encapsulated IAA (LNPs-IAA) [0.05 and 100 μg/mL], and IAA solutions [0.05 and 100 μg/mL]. IAA (Sigma-Aldrich, Brazil) was dissolved in potassium hydroxide (Sigma-Aldrich, Brazil) and distilled water, resulting in a final volume of 100 mL.

The treatments were applied twice, with a 15-day interval between each application for each species. The first application occurred on the 10th day after sowing, and the second on the 25th day. The solutions were applied using a manual sprayer at 9 a.m., with a final volume of 50 mL, ensuring complete leaf coverage, with each plant receiving 5 mL. Every day at 5 p.m., a stem segment located 0.5 mm from the transition zone was collected and prepared for anatomical analyses from each species. For wheat, we considered the stem as the region where adventitious roots emerge from the primary point. This procedure was repeated for 35 days after germination. In total, 25 days of sampling were conducted, including a control sample from each treatment, which was collected and analyzed before the first application on the 9th day.

2.4. Growth conditions

Under the experimental conditions, 50 seeds of each species were sown in 5 L pots for each treatment. Throughout the 35-day experiment, the plants were maintained in a greenhouse with regular irrigation at five intervals (07:00, 10:00, 13:00, 16:00, and 18:00) for 2 min per session, with a total water volume of 5225 mL distributed across five sprinklers. The experiments were conducted between June and July, corresponding to late autumn and winter. The temperature values (maximum, average, and minimum) and relative humidity (%) inside the greenhouse are presented in Supplementary Figure 01.

2.5. Anatomical analysis

To evaluate possible anatomical structural changes, the stem samples collected as previously described were fixed in neutral formalin for 48 h. The samples were then dehydrated with 70 % alcohol and stored in glass containers. Subsequently, the stem portions were further dehydrated with 100 % alcohol and infiltrated with hydroxyethyl methacrylate (Leica Historesin®, Heraeus Kulzer, Germany). The resulting blocks were sectioned using a rotary microtome (Leica Biosystems, RM 2045, Germany) into transverse sections with a thickness of 5 –7 μm. The sections were stained with 0.05 % toluidine blue in phosphate-citric acid buffer at pH 4.5 and mounted on slides with coverslips using synthetic resin (Entellan®, Merck, Germany). The results were documented through image capture using an Olympus DP71 video camera attached to an Olympus BX 51 microscope.

2.6. Biometric anatomical analysis

To assess the influence of auxin on xylem development, the following variables were measured: the total number of vessels, total xylem area (mm^2), cambial zone thickness (μm), primary thickness meristem (Ptm), and equivalent vessel diameters (μm).

For the cherry tomato, the total area of the vascular cylinder was measured, excluding the pith and phloem portions (See Figure 01a). For wheat, all vascular cylinders were measured, as xylem tissue is formed within vascular bundles along with phloem and parenchymal cells (See Figure 01b). These results were recorded in μm^2 and converted to mm^2.

Regarding vessel number, all fully differentiated vessels were counted, while undifferentiated vessels were excluded. The equivalent diameter (De) was calculated follow the methodology described by Scholz (Scholz et al., 2013), with 50 vessels measured per sample. In the initial evaluation days, all vessels were measured. Cambial zone thickness was measured only in the cherry tomato. The cambial zone (Cz) was defined as the layers where no clear differentiation into xylem or phloem cells was observed. In wheat, instead of the cambial zone, the primary thickness meristem (Ptm) was measured.

2.7. Confocal microscopy analysis

The LNPs were labeled with Liss Rhod PE (1,2-dioleoyl-sn-glycero-3-phosphoethanolamine-N-(lissamine rhodamine B sulfonyl) (ammonium salt) for localization analyses. For this purpose, samples of each species received a solution containing labeled lignin nanoparticles on the 20th day after sowing. The applied solution volume was 50 mL per species. Spraying was performed using a manual sprayer, ensuring complete coverage of all expanded leaves, with each plant receiving between 3 and 5 mL of the solution. Control plants were included, receiving only distilled water.

Samples of stem were collected at 1, 2, 4, and 8 h after the application of the labeled LNP solution. The collected plants were fixed in 4 % paraformaldehyde for 4 h, followed by washing in phosphate buffer and distilled water. Subsequently, transverse sections were examined. Under the microscope, two different channels were used: one for autofluorescence and transmitted light imaging, and the other for detecting the specific wavelength range of the fluorochrome in green. The excitation wavelength used was 552 nm, with emission detected between 572 nm and 607 nm for the fluorochrome, and between 430 nm and 660–680 nm for autofluorescence (Fig. 1a, f, k). The images presented in this study are composed of a combination of both channels, providing a comprehensive visualization of the samples. Characterization for LNP in water are presented in Supplementary Figure 2b.

2.8. Statistical analysis

To test the influence of the treatments on xylem development over time, the anatomical quantitative data were analyzed using GLM (linear generalized model) with a gamma family distribution, without interactions, to determine whether the treatments independently influenced xylem area, cambial zone thickness, Ptm thickness, as well as the number and diameter of vessels, with the water treatment as the reference. Additionally, we applied a GLM model with an interaction between day and treatment to assess whether the application day influenced xylem growth differently, using the water treatment as the reference. Finally, we conducted a correlation and multivariate analysis (PCA) to better understand the behavior of each treatment concerning in relation to the measured variables. All analyses were performed using R software.

To calculate the percentage increases in xylem quantitative parameters, we used the coefficients obtained from the GLM models. The treatment coefficients represent logarithmic effects, which were converted into percentage increases (%) using the equation 01, where β is the estimated coefficient for each treatment. These calculations provide

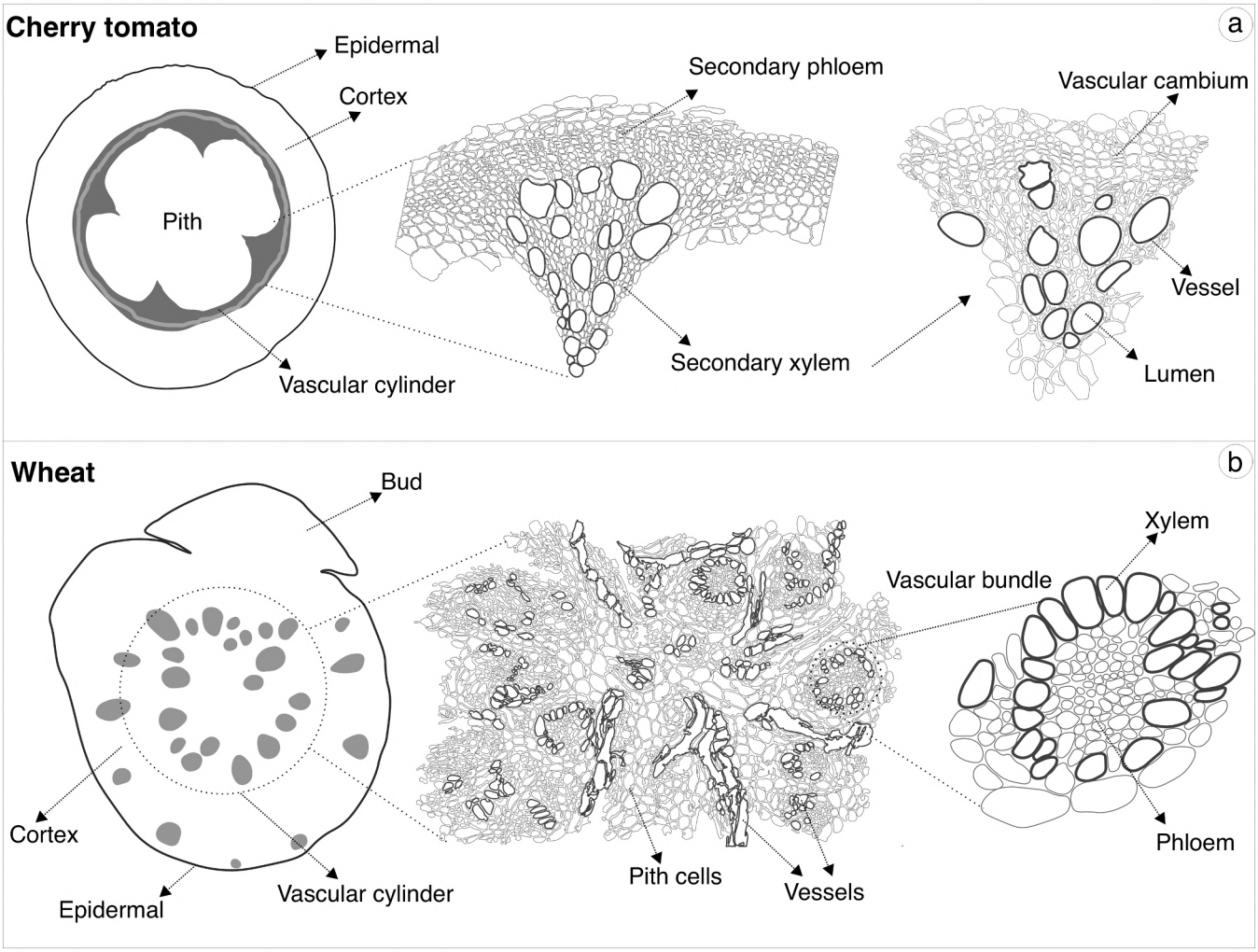

Fig. 1. Schematic representation of transverse sections of stem regions in cherry tomato and wheat. (a) Detail of the vascular cylinder in cherry tomato, highlighting the secondary xylem within the vascular bundles. In this species, the vascular cylinder area was measured excluding the portions corresponding to the pith and secondary phloem. (b) Detail of the stem region in wheat, showing the central vascular cylinder and the vascular tissues organized in scattered bundles. In this species, the calculation of the vascular cylinder area included both the cells composing the pith and the phloem tissue.

an estimate of the percentage increase relative to the control for each individual treatment.

$$(e^{\beta} - 1) \quad \times 100 \tag{1}$$

3. Results

3.1. Characterization of LNP, LNP-IAA and LNP-labeled

Lignin nanoparticle size, polydispersity index, and zeta potential values are presented in supplementary table 1. The lignin nanoparticles (LNPs) exhibited an encapsulation efficiency of 90 % for indole-3-acetic acid (IAA) (see Supplementary Table 2 for detailed data). The IAA release profile revealed that LNP-IAA released approximately 52 % of the encapsulated phytohormone within 24 h, whereas 100 % of free IAA was released during the same period (Supplementary figure 02a).

3.2. Localization of labeled LNP

Lignin nanoparticles (LNP) exhibited rapid uptake and distinct spatiotemporal distribution patterns in cherry tomato plants following foliar application. Within just one hour post-treatment, LNP were already detectable in the cortical region, primarily localized in the cellular apoplast (Fig. 2b). Concurrently, nanoparticles had reached the vascular cylinder, where they were observed both within parenchyma cells and associated with xylem vessel walls. Between 2 and 4 h post-application (Fig. 2c, d), LNP presence decreased in these initial regions but persisted in the medullary region and maintained association with vascular elements. By 8 h (Fig. 2e), cortical detection became negligible while vascular localization patterns shifted, with LNP remaining specifically within vessel elements - both along their walls and in the cambial zone. Notably, epidermal cells retained LNP throughout all evaluation periods (Fig. 2b-d), suggesting these surface cells may serve as both entry points and reservoirs for nanoparticle accumulation.

In wheat plants, LNP exhibited uptake and distribution dynamics comparable to tomato, though with some distinct anatomical features (Fig. 2 g). Similar to tomato, cortical presence peaked at 1 h post-application (Fig. 2 g) before progressively declining at 2 h (Fig. 2 h), 4 h (Fig. 2i), and 8 h (Fig. 2j). The nanoparticles localized primarily in the cortical apoplast but were also detected intracellularly within cortical parenchyma cells (Fig. 2 h). However, vascular distribution patterns differed - while LNP clearly associated with vascular bundle parenchyma (Fig. 2 g), their specific interaction with xylem vessel walls remained ambiguous. Notably, adventitious roots emerged as significant sites for nanoparticle absorption (Fig. 2k-o), suggesting these structures may provide alternative entry pathways in wheat. Our observations

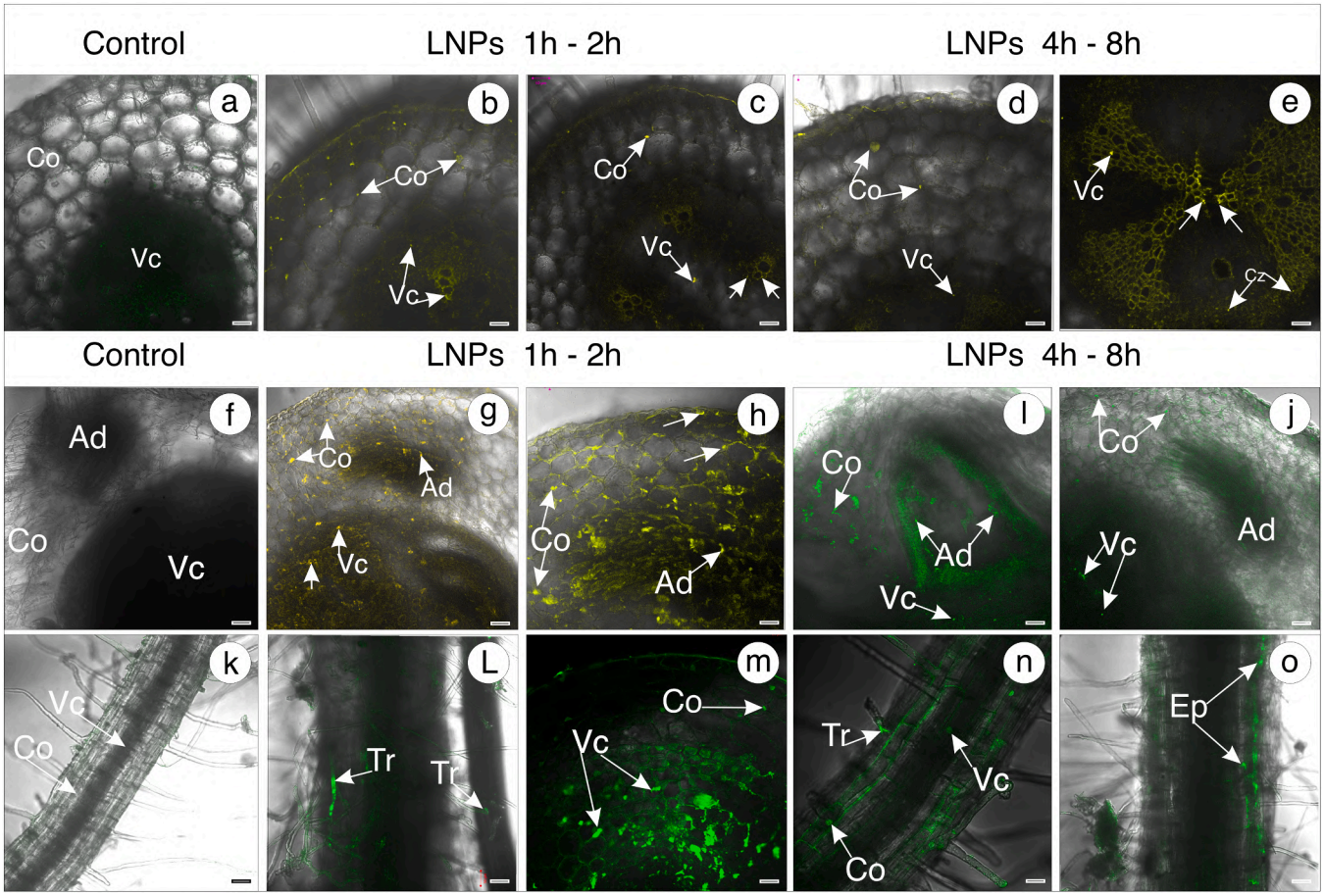

Fig. 2. Confocal micrographs of the stem region in cherry tomato (a–e) and wheat (f–o), showing the presence of lignin nanoparticles (LNP) labeled with Rhodamine B. In tomato and wheat, hand-cut transverse sections of the stem region were analyzed. Especially in wheat, we observed a significant role of root hairs and adventitious roots in the internalization of LNP (k-o). Ad = adventitious root;Co = cortex; Cz = cambial zone; Ep = epidermis; Vc = vascular cylinder;St = stomata. Scale bars: 20μm.

indicate that root hairs (Fig. 2 L) on adventitious roots mediate both adhesion and potential absorption of LNP. When examined in isolation, adventitious roots showed the presence of LNP in cortical tissues (Fig. 2 m) and vascular cylinders (Fig. 2 n) within just 2 h post-application. Remarkably, LNP persisted in epidermal regions even after 8 h (Fig. 2o), demonstrating prolonged retention at the root-soil interface.

3.3. Development of the vascular cambium and primary thickness meristem (ptm)

Our comprehensive analysis encompassed an average of 450 stem anatomical sections across tomato and wheat, capturing the complete developmental progression of xylem tissue from day 10 post-sowing onward. Figs. 4a and 5a collectively provide a complete visualization of this growth trajectory, revealing both conserved and species-specific patterns of xylem differentiation.

In cherry tomato plants, cambial development followed a precise ontogenetic sequence across all treatments (Fig. 3a, 10th – 25th). The fascicular cambium initiated between primary xylem and phloem on day 10th, achieving complete establishment by day 14th, during which only anticlinal divisions occurred in medullary parenchyma. A distinct developmental phase began on day 14 with the formation of intra-fascicular cambium between vascular bundles. This progression continued until day 16th, when fascicular cambium maturation was completed. The interfascicular cambium starts the cell differentiation between the 18th and 20th day. Notably, treatment effects became apparent in later stages - while control and LNP 100 μg/mL plants required until day 25th for full vascular cylinder cambium establishment, all other treatments with IAA presence showed accelerated development, achieving this by day 23rd. Histological analysis revealed functional differentiation wherein the fascicular cambium generated secondary xylem (inward) and phloem (outward), while the inter-fascicular cambium produced only specific secondary xylem cells: (i) lignified fibrous cells, (ii) parenchymatic rays centripetally, and (iii) secondary phloem centrifugally.

In wheat, vascular cylinder differentiation (Fig. 3b, 10th–25th) initiates with procambial-derived vascular bundles forming at the center of the pith. No primary thickening meristem (PTM) establishment was detected before day 10th after sowing. Notably, LNP and IAA 100 μg/mL treatments exhibited PTM cell differentiation encircling the vascular cylinder by day 12th, while other treatments showed this differentiation only from day 14th. During organ growth, central procambial strands developed exclusively into amphivasal vascular bundles. Neither free nor encapsulated IAA application significantly affected this cellular differentiation. PTM activity typically generated amphivasal bundles (Fig. 5 f) between days 18th– 22th, with LNP-IAA and IAA 100 μg/mL treatments demonstrating earlier PTM activation (18th) compared to other treatments (20th). Moreover, in the control treatment, no tillering process was observed (Fig. 5a), whereas all other treatments exhibited tillering at different time points. In the IAA 100 μg/mL treatment, tillering began at 21 days; in LNP 100 and LNP-IAA 100 μg/mL, at 25 days; and in LNP-IAA 0.05 and IAA 0.05 μg/mL treatments, at 27 days.

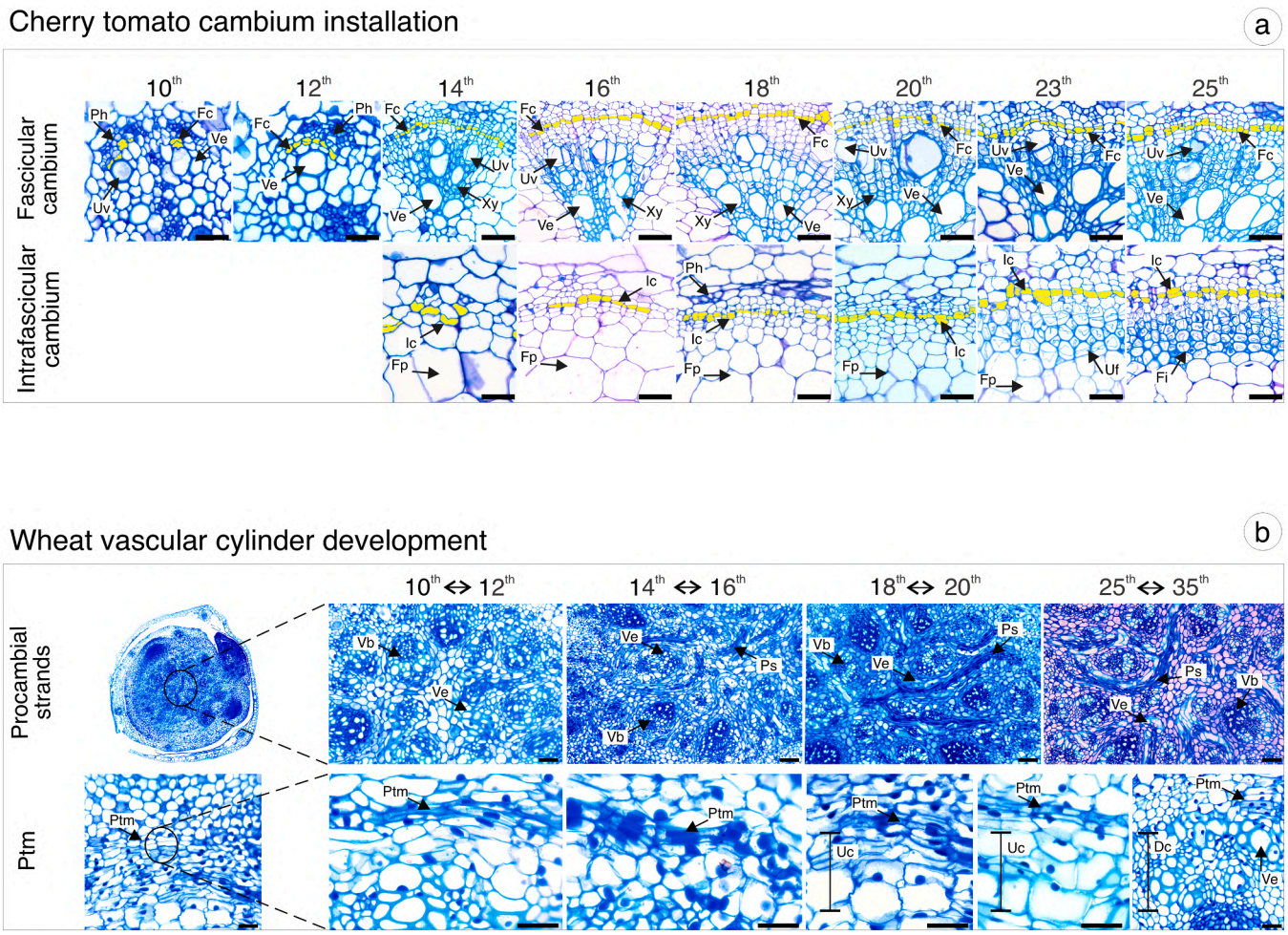

Fig. 3. Comparative vascular cylinder anatomy across species: Transverse sections of cherry tomato and wheat showing developmental progression of vascular cambium establishment and primary thickening meristem (PTM) activity during the experimental period. Note: Yellow staining in cherry tomato sections serves as an artificial visual aid for cambial zone identification and does not represent native cellular staining properties. Dc = differentiated cells; Fp = ground parenchyma; Fc = fascicular cambium; Ic = interfascicular cambium; Ph = phloem; Ptm = primary thickening meristem; Ps = procambial strands; Uv = undifferentiated vessels; Ve = vessels; Xy = xylem. Scale bars: a = 100 μm. b = 200 μm.

3.4. Cherry tomato: xylem quantitative traits

Analysis of the xylem development revealed distinct temporal responses to foliar treatments (Fig. 4a). Following the first foliar application, total xylem area (Fig. 4b) showed detectable differences only by day 8, whereas vessel number (Fig. 4 f) and diameter (Fig. 4 h) diverged as early as day 3. Cambial zone thickness (Fig. 4d) responses were immediate, with alterations visible on the application day across all treatments. The second application triggered accelerated responses: LNP-IAA (both concentrations) and free IAA 100 μg/mL induced significant xylem expansion by 8 h after application, followed by IAA 0.05 μg/mL and LNPs by day 3. Vessel number increased in all treatments except controls, with LNP-IAA 100 μg/mL showing the most pronounced effect. The vessel diameter remained largely unaffected, except for LNP 100, which showed a significant post-reduction after the second application. Cambial zone dynamics revealed contrasting trends – IAA treatments decreased thickness, while LNP-IAA and controls initially increased it before subsequent reduction in all groups post-application. Notably, all treated plants exhibited statistically significant xylem expansion compared to controls (Supplementary Table 02).

Foliar application of LNP-IAA at 0.05 μg/mL elicited the most pronounced enhancement in xylem area (95.3 % increase), closely followed by IAA 0.05 μg/mL (93.4 % increase) (Fig. 4b). The nanoparticle treatments demonstrated concentration-dependent efficacy, with LNP alone increasing xylem area by 67.7 %, while the higher concentration LNP-IAA 100 μg/mL showed more modest effects (32 % increase). Free IAA at 100 μg/mL yielded intermediate results (a 55.3 % increase).

Analysis of cambial zone responses revealed distinct treatment-specific effects. Both IAA formulations (0.05 and 100 μg/mL) significantly reduced cambial thickness by approximately 40 %, while LNP-IAA treatment showed a slightly less pronounced effect (32 % reduction). Other treatments exhibited no measurable impact on cambial dimensions. All treatments except LNP significantly influenced vessel characteristics compared to the control (Fig. 4 f, h). For vessel number, the 100 μg/mL IAA and LNP-IAA treatments showed the strongest effects, increasing vessel density by 37.6 % and 33.2 %, respectively. The lower concentration treatments (0.05 μg/mL) also enhanced vessel formation, though to a lesser degree, with IAA producing a 27.1 % increase and LNP-IAA a 22.2 % increase.

3.5. Wheat: cylinder vascular quantitative traits

Similar to observations in cherry tomato plants, analysis of the xylem development revealed distinct temporal responses to foliar treatments (Fig. 5a). Following initial application, xylem area (Fig. 5b) demonstrated significant differences beginning at day 5. Vessel number (Fig. 5d) responded most rapidly to LNP-IAA 0.05 μg/mL, showing significant changes by day 2, while other treatments exhibited delayed

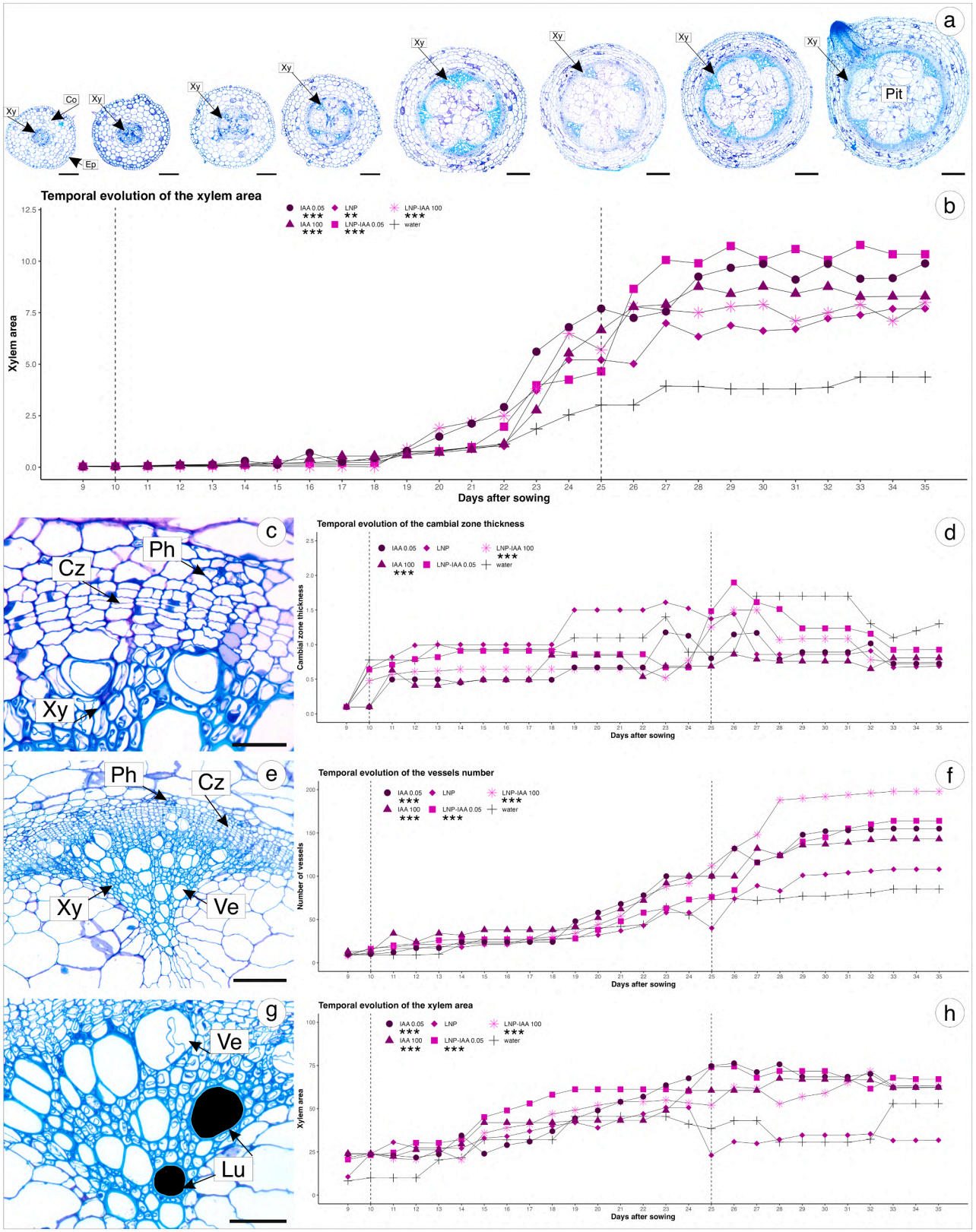

Fig. 4. Anatomical and quantitative characterization of secondary xylem development in cherry tomato. The dashed lines represent the days of treatment application. (a) Temporal progression of xylem formation shown in daily transverse stem sections. (b) Quantitative expansion of xylem area over the experimental period. (c) Vascular bundle anatomy highlighting cambial zone organization. (d) Cambial zone thickness dynamics throughout development. (e) Representative vascular bundle cross-section. (f) Chronological changes in xylem vessel number. (g) High-resolution vascular bundle section showing secondary xylem vessels (lumen areas in black). (h) Calculated vessel equivalent diameters derived from lumen area analyses.Co = cortex; Cz = cambial zone; Ep = epidermis; Lu = lumen; Ph = phloem; Pit = pith; Vb = vascular bundle; Ve = vessels; Xy = xylem. Scale bars: a = 500 μm. e = 200 μm. g = 100 μm. c = 50 μm. Significance code: *** = 0.001. ** = 0.01. * = 0.05.

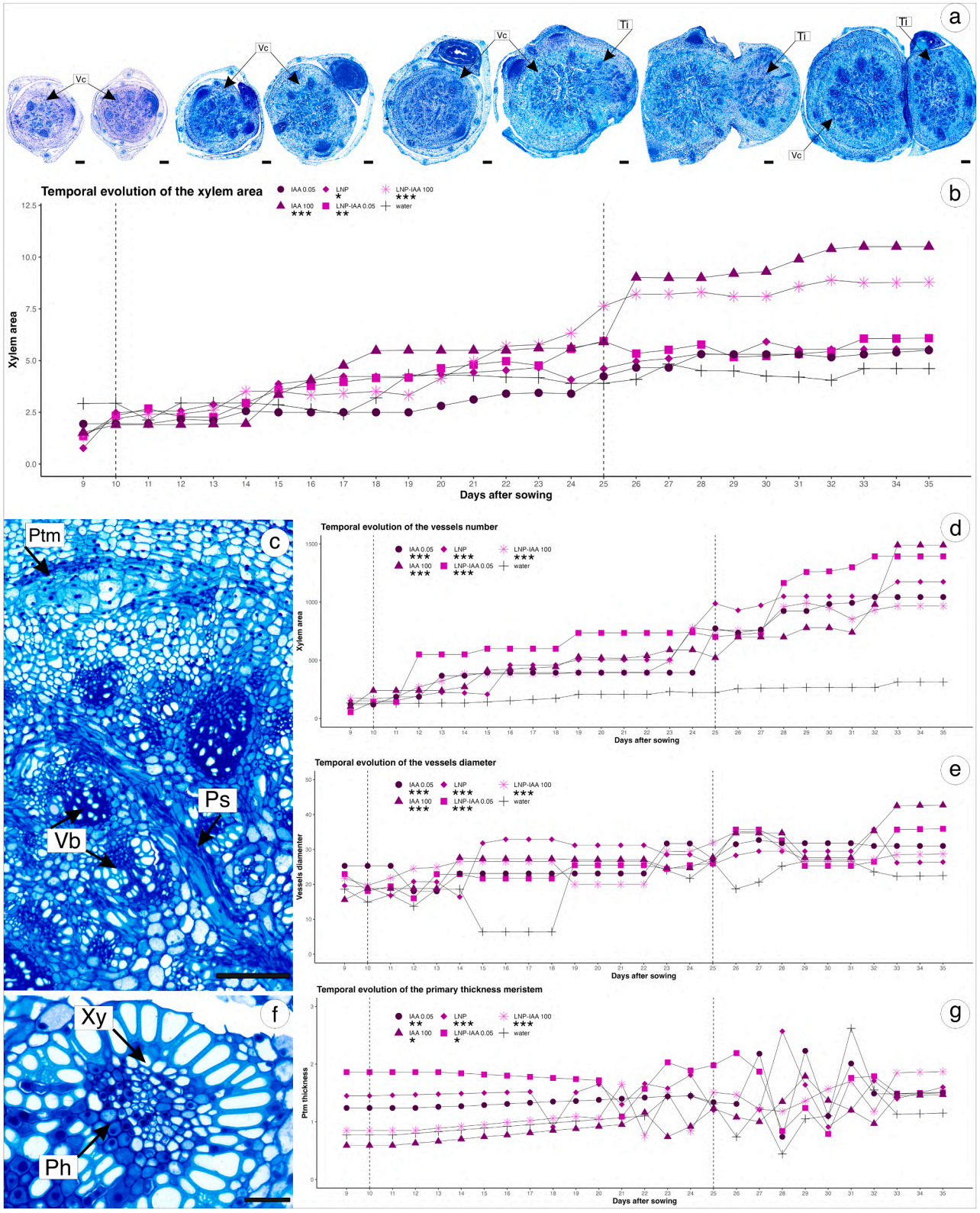

Fig. 5. Anatomical and quantitative characterization of cylinder vascular development in wheat. The dashed lines represent the days of treatment application. (a) Daily transverse stem sections showing vascular cylinder development during the experimental period. (b) Temporal expansion of vascular cylinder area. (c) Anatomical detail of vascular cylinder organization, highlighting the primary thickening meristem (PTM) zone. (d) Dynamics of xylem vessel number over time (e) Calculated vessel equivalent diameter derived from lumen area measurements. (f) Representative vascular bundle cross-section. (g) PTM zone thickness progression across developmental stages. Ph = phloem. Ptm = primary thickness meristem. Ps = procambial strands. Vb = vascular bundle. Ti = tiller. Vc = vascular cylinder. Xy = xylem. Scale bars: a = 500 μm. c = 200 μm. f= 50 μm. Significance code: *** = 0.001.** = 0.01. * = 0.05.

responses (day 4 +). Vessel diameter (Fig. 5e) displayed later developmental effects, with significant variation emerging only after day 5. Primary thickening meristem (PTM) remained unaffected throughout the initial phase (Fig. 5 g). Following the second application, xylem area increased significantly only in the LNP-IAA and IAA 100 μg/mL treatments, with no effect observed in others. Vessel number responded immediately in LNP-IAA 0.05 μg/mL and LNP treatments, while IAA 100 μg/mL showed delayed increases (day 5), and other treatments exhibited only marginal changes. No significant treatment effects were detected for vessel diameter. In contrast, primary thickening meristem (PTM) decreased across all treatments, though the magnitude of reduction varied by treatment type.

The vascular cylinder area (Fig. 5b) increased by 45 % and 43 % following treatment with IAA and LNP-IAA at 100 μg/mL, respectively. Among the 0.05 μg/mL treatments, only LNP-IAA showed a significant increase of 21 %, while IAA at the same concentration had no effect. Similar to the results observed in cherry tomato, LNP at 100 μg/mL promoted an 18 % increase in vascular cylinder area. All data are presented in Supplementary Table 03.

All treatments significantly influenced xylem vessel development, affecting both vessel number (Fig. 5d) and diameter (Fig. 5e). The LNP-IAA 0.05 μg/mL treatment showed the most pronounced effect on vessel proliferation, increasing vessel number by 258 %, followed by LNP 100 μg/mL (182 % increase), both free IAA treatments (150 %), and LNP-IAA 100 μg/mL (127 %). Regarding vessel diameter, LNP 100 μg/mL caused the greatest expansion (40 % increase), closely followed by both 100 μg/mL formulations (37 %) and the 0.05 μg/mL treatments (~30 %). While most treatments showed stable diameter effects over time, LNP-IAA 100 μg/mL uniquely induced a gradual reduction in vessel diameter. All data are presented in Supplementary Table 03.

3.6. Interaction between days and treatment

In these analyses, we evaluated the effects of both time (days post-application) and treatment type on growth rates. For cherry tomato, the control group exhibited an average daily growth rate of 18.4 %. Application of IAA at 0.05 μg/mL resulted in a slight increase in this rate, while the higher IAA concentration (100 μg/mL) led to a slightly lower rate than the control; however, neither of these differences was statistically significant (Table 2). Application of isolated nanoparticles (LNP 100) significantly increased the daily growth rate. The most pronounced effects were observed in the treatments combining LNP with IAA (LNP-IAA 0.05 and LNP-IAA 100), both of which showed statistically significant increases compared to the control (Table 2).

In wheat (Supplementary Table 04), results showed that the control group had an average daily growth rate of approximately 3.98 %. Application of IAA at 0.05 μg/mL led to a slight, non-significant increase in growth rate. In contrast, IAA at 100 μg/mL significantly enhanced daily growth. Among the nanoparticle treatments, LNP 100 did not significantly alter the growth rate. However, the combined LNP and IAA treatments had more pronounced effects and showed the greatest increase among all treatments, which was statistically significant (Table 2).

Table 1
Characterization of lignin nanoparticles (LNP), lignin nanoparticles encapsulating IAA (LNP-IAA) and labeled LNP performed using dynamic light scattering (DLS). PDI refers to the polydispersity index.

	Size (nm)	PDI	Zeta Potential (Mv)
LNP	201 ± 85	0.151	-34.5
LNP-IAA	221 ± 70	0.166	-41.7
Labeled-LNP	228 ± 3.4	0.290	-50.0

Table 2
Generalized Linear Model (GLM) with interactions between days and treatments on xylem area growth in cherry tomato and vascular cylinder growth in wheat.

Xylematic area	Coefficient (log)	Standard error	p-value	Daily growth	Significance
Intercept	-4.60253	0.24243	$< 2e^{-16}$		***
Days	0.16895	0.01092	$< 2e^{-16}$	18.4 %	***
Days: IAA 0.05	0.01457	0.01544	0.3470	20.1 %	
Days: IAA 100	-0.00348	0.01544	0.8220	17.9 %	
Days: LNP 100	0.02625	0.01544	0.0203	**21.5 %**	*
Days: LNP-IAA 0.05	0.03628	0.01544	0.0202	**22.8 %**	*
Days: LNP-IAA 100	0.03485	0.01544	0.0256	**22.6 %**	*
Cylinder vascular area	Coefficient (log)	Standard error	p-value	Daily growth	Significance
Intercept	0.338142	0.133004	0.012115		*
Days	0.039804	0.005990	$6.47e^{-10}$	3.98 %	***
Days: IAA 0.05	0.009589	0.008471	0.259623	4.94 %	
Days: IAA 100	0.033578	0.008471	0.000118	**7.34 %**	***
Days: LNP 100	-0.002828	0.008471	0.738976	3.70 %	
Days: LNP-IAA 0.05	0.005717	0.008471	0.500903	4.55 %	
Days: LNP-IAA 100	0.038049	0.008471	$1.48e^{-05}$	**7.78 %**	***

3.7. Correlation and principal component analysis (PCA)

In cherry tomatoes, the xylem area showed a strong positive correlation with xylem vessel number (Fig. 6a), with all treatments exhibiting correlation coefficients greater than 90 %. However, the relationship between xylem area and cambial zone thickness (Fig. 6c) revealed treatment-specific patterns: the LNP treatment demonstrated a negative correlation, while other treatments showed moderate correlations ranging from 50 % to 70 %. The principal component analysis revealed that the selected components accounted for 93 % of the total data variability in cherry tomatoes (Fig. 6e). The control treatment showed no significant correlations with any of the measured variables. The LNP 100 μg/mL treatment exhibited minimal association solely with the cambial zone. Notably, distinct treatment-specific patterns emerged: LNP-IAA 0.05 μg/mL demonstrated a strong positive correlation with xylem area, while IAA 0.05 μg/mL significantly influenced vessel number and diameter. The IAA 100 μg/mL treatment showed weak correlation with vessel number and no association with other parameters, whereas LNP-IAA 100 μg/mL was specifically correlated with vessel number. Importantly, the cambial zone displayed no significant relationship with any xylem characteristics, including vessel parameters and total xylem area, suggesting its developmental independence from these vascular features.

In wheat, vascular cylinder area showed strong correlation with xylem vessel number across all treatments (Fig. 6b). Primary thickening meristem (PTM) thickness, however, exhibited considerable treatment-dependent variation (Fig. 6d). Mirroring the cherry tomato results, the LNP 100 μg/mL treatment showed weak correlation (~10 %). Notably, the LNP-IAA 0.05 μg/mL treatment displayed a negative correlation, contrasting with the strong correlations observed for 100 μg/mL concentrations. The control and IAA 0.05 μg/mL treatments both demonstrated similarly low correlation coefficients. Principal component analysis accounted for 91 % of the data variability in wheat (Fig. 6 f). Both IAA and LNP-IAA at 100 μg/mL concentrations showed strong positive correlations with xylem area, while their 0.05 μg/mL counterparts primarily influenced vessel number. Notably, none of the

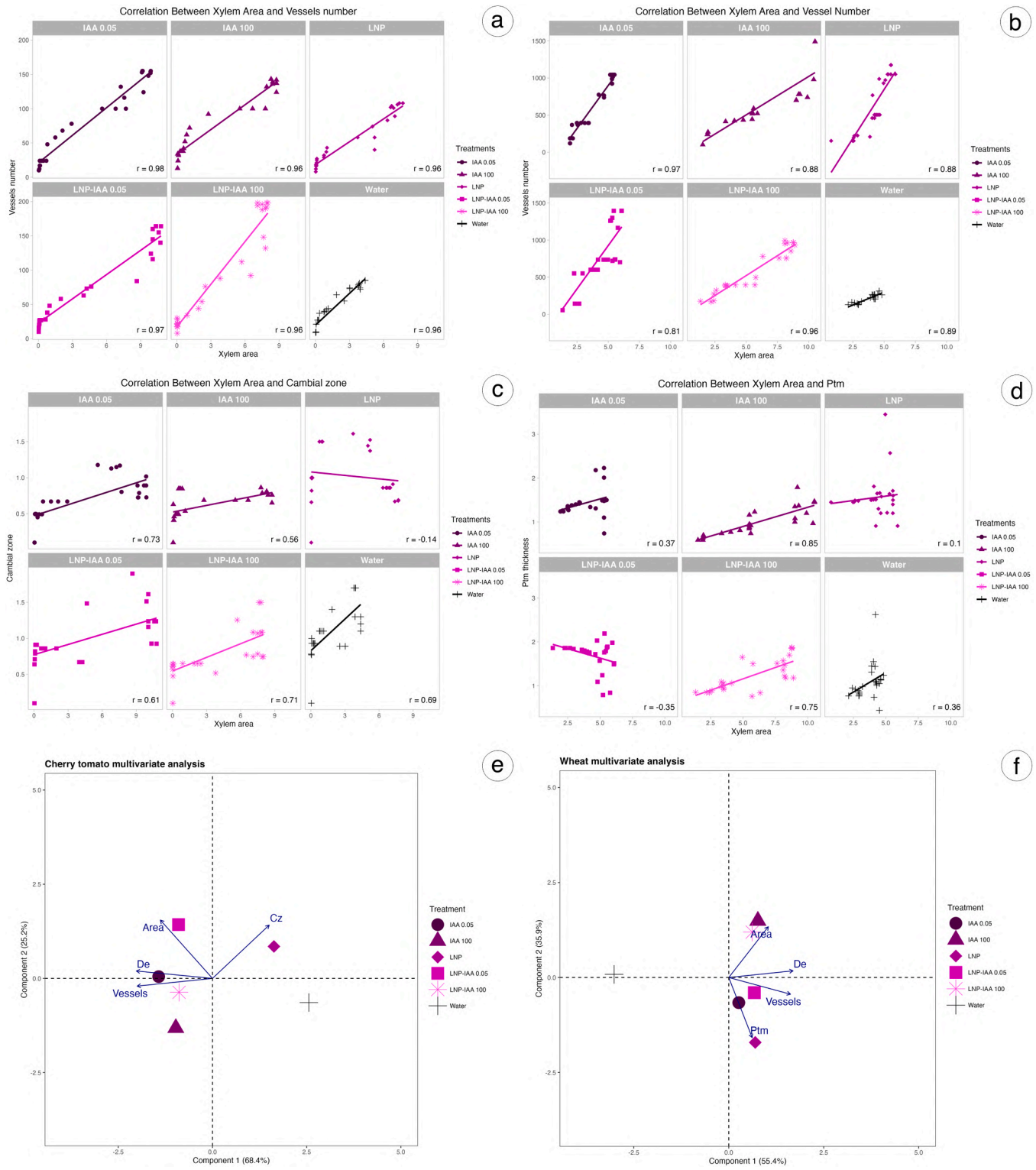

Fig. 6. Correlation and principal component analyses of xylem quantitative parameters under the applied treatments in cherry tomato (a, c, e) and wheat (b, d, f). Cz = cambial zone; De = equivalent diameter; Ptm = primary thickness meristem.

treatments had a significant effect on vessel diameter. The LNP 100 μg/mL treatment demonstrated a marked association with the primary thickening meristem activity, contrasting with the control treatment, which showed no significant correlations. Interestingly, while the primary thickening meristem displayed no relationship with xylem area (consistent with observations in cherry tomato), it maintained a significant correlation with vessel number.

4. Discussion

The results demonstrate that lignin nanoparticles (LNPs) were efficiently absorbed and systemically distributed through the vascular systems of both plant species. The kinetics and intensity of internalization showed minimal variation between species. In terms of stem development, pronounced morphological alterations were detected in xylem

tissue organization. These structural modifications were primarily influenced by three factors: (1) the concentration of applied LNP–IAA and free IAA, (2) application frequency, and (3) plant species. The LNP–encapsulated IAA formulation promoted significantly greater daily increases in xylem growth compared to the controls in both species. Notably, even unloaded LNPs induced measurable changes in growth parameters, indicating nanoparticle-specific biological effects that extend beyond hormone delivery.

The absorption and systemic translocation of nanoparticles (NPs) are fundamental determinants of their efficacy in nanotechnology-based agricultural applications (Zhang et al., 2023). Although particle size can influence encapsulation efficiency and release kinetics where smaller LNPs often promote faster release due to higher surface area to volume ratios the release profile is primarily determined by the molecular interactions within the nanoparticle matrix and can be further modulated by composition, preparation method, and environmental conditions (Beach et al., 2024). Precise characterization of uptake pathways and kinetic profiles is therefore essential for optimizing nanocarrier performance.

Although early research on NP absorption primarily focused on inorganic nanoparticles, recent studies have shown that polymeric NPs can also undergo foliar uptake, mainly through stomatal penetration (Avellan et al., 2021). This process is strongly influenced by both plant-related factors (such as morphophysiological traits) and NP physicochemical properties, including size, surface charge, and chemical composition (Rani et al., 2023). Specifically for lignin nanoparticles (LNPs), recent evidence indicates multiple internalization routes, including seed coat permeation (Faleiro et al., 2025) and absorption via the Poaceae root system (Falsini et al., 2020).

Our results corroborate previous findings, showing that lignin nanoparticles (LNPs) are rapidly absorbed by both cherry tomato and wheat, with clear evidence of localization within the vascular cylinder as early as one hour after exposure. This observation confirms their immediate potential for systemic translocation. Although morphological and physiological differences among botanical groups are often cited as factors influencing nanoparticle absorption, the present study demonstrates that LNPs display a consistent uptake pattern across both monocot (wheat) and eudicot (cherry tomato) species (Spielman-Sun et al., 2019; Sun et al., 2014).

Furthermore, this work provides the first evidence of LNP accumulation in stem tissues following foliar application, confirming not only the effectiveness of the delivery route but also the ability of these nanoparticles to translocate from the leaf surface into the vascular regions, a process commonly reported for other NP types (Sun et al., 2014; Zhu et al., 2021, 2020).

In addition to foliar uptake, LNP accumulation was also detected in the adventitious roots of wheat, suggesting that these structures may contribute to nanoparticle absorption and subsequent translocation. Previous studies have confirmed that lateral and adventitious roots act as primary entry points for soil-applied nanoparticles (Avellan et al., 2021; Wang et al., 2023), including in wheat (Cifuentes et al., 2010). However, root-mediated internalization is strongly constrained by particle size. The endodermal barrier, characterized by Casparian strip deposition along the anticlinal walls (Evert, 2013), substantially restricts apoplastic translocation of nanoparticles into the vascular cylinder. As reported by Azim et al. (2023), this specialized cellular structure represents a major bottleneck for root-to-shoot nanoparticle transport, particularly for larger particles. Our findings are consistent with this mechanism, showing LNPs predominantly localized within the root cortex and with limited association to the vascular cylinder.

Finally, our localization analyses revealed that foliar-applied LNPs successfully penetrate internal stem tissues, including the cortical region and the vascular cylinder. This penetration is essential for the effective delivery of bioactive compounds to zones of active cell division and differentiation. The confirmed presence of nanoparticles within these compartments provides mechanistic support for the significant effects observed in xylem parameters. These structural alterations reflect the complex interplay between treatments using LNPs, LNP–IAA, and free IAA, as well as the underlying processes of vascular differentiation. Notably, the observed modifications were not uniform but rather dependent on multiple factors, revealing a dose- and context-dependent response that suggests both stimulatory and inhibitory effects.

Our results demonstrate that both free IAA and IAA encapsulated in LNPs accelerated the differentiation of the vascular cambium and the primary thickening meristem (PTM) by approximately two days compared to the control. This suggests that the initial application during the juvenile phase (10 days after sowing) promoted the early establishment of these meristematic tissues. The differentiation of meristems responsible for vascular development, particularly xylem formation, is regulated by a complex hormonal network in which auxins play a central role (Bhalerao and Fischer, 2017; Milhinhos and Miguel, 2013).

The mechanism of auxin action involves: (i) polar transport mediated by PIN transporters —particularly PIN6 — which establish radial spatial gradients (Simon et al., 2016); (ii) modulation by AUX/LAX regulatory genes, especially LAX2, which maintain hormonal homeostasis and ensure precise control of xylem expansion (Moreno-Piovano et al., 2017); and (iii) signaling cascades that activate genes associated with other growth regulators, mainly cytokinins and gibberellins (Yang and Zhu, 2022). These auxin gradients function as dynamic positional signals, showing peak concentrations in cambial cells, gradually decreasing in differentiation zones, and becoming absent in mature xylem (Yang and Zhu, 2022). Such gradients temporally and spatially coordinate cambial differentiation and subsequent cell division (Xu et al., 2019). Consequently, polar auxin gradients act as key positional cues for vascular organization, regulating both cell proliferation and specialization (Aloni, 2013; Milhinhos and Miguel, 2013). Alterations in endogenous auxin concentrations modify efflux and influx dynamics, promoting the differentiation of procambial and cambial cells (Ye, 2002) and enhancing rates of cell division and differentiation, mechanisms that align with the stimulatory effects observed following exogenous hormone application (Aichinger et al., 2012; Sanchez et al., 2012).

Despite the early activation of meristems, our data indicate that the thickness of these tissues (cambium and PTM) is not directly correlated with xylem expansion, as little to no statistical association was detected. This finding suggests that xylem expansion is governed not merely by meristematic mass but instead by the intensity of mitotic activity and localized hormonal signaling.

While the first application primarily influenced the establishment of vascular meristems, the second application significantly enhanced quantitative parameters, eliciting measurable responses within as little as eight hours. The contrasting outcomes between the two applications underscore the importance of the phenological stage at which the hormone is applied.

The second application, performed at a more advanced developmental stage, triggered faster and more robust responses, consistent with studies reporting greater effectiveness of growth regulators when applied across multiple growth phases — both vegetative and reproductive (Dubey et al., 2024; Janmohammadi and Sabaghnia, 2023; Pham et al., 2023; Shahsavar et al., 2024). This pattern aligns with findings in maize, where treatments administered at later stages resulted in higher productivity compared to juvenile and control plants (Xu et al., 2024), reinforcing the critical role of application timing in maximizing plant response.

Both species exhibited clear and significant responses to the treatments. In tomato, we observed an increase in total xylem area, whereas in wheat, we detected an expansion of the vascular cylinder. Treatment efficacy was distinctly species- and concentration-dependent: in cherry tomato, LNP–IAA at 0.05 μg mL^{-1} induced the greatest xylem expansion, followed by free IAA at the same concentration. In contrast, in wheat, free IAA at 100 μg mL^{-1} produced the strongest effect, with LNP–IAA at 100 μg mL^{-1} showing slightly lower performance. These trends were

consistently supported by both linear modeling and multivariate analyses. Recent studies have demonstrated that auxin gradients determine the spatial positioning of vascular meristems and that exogenous hormone applications can stimulate differential patterns of cell division and expansion by elevating endogenous auxin concentrations (Bhalerao and Fischer, 2017; Eswaran et al., 2024; Růžička et al., 2015).

These findings are consistent with several reports in the literature. In Arabidopsis and sunflower, IAA treatments increased stem xylem area and were positively correlated with higher grain yield (Cabello and Chan, 2019), (with vascular bundle induction detected as early as seven hours after application, a pattern similar to that observed in our study. In Populus, the synergistic interaction between IAA and gibberellins resulted in a threefold increase in xylem area compared with individual treatments (Björklund et al., 2007). Likewise, in cherry tomato, seed-based application of LNP–IAA produced a dose-dependent response: higher concentrations promoted greater stem xylem expansion, whereas lower concentrations primarily modulated root development (Faleiro et al., 2025). Collectively, these findings emphasize that the method of hormone delivery (foliar vs. seed treatment) elicits distinct morphogenetic responses and reinforce the positive correlation between xylem expansion and vessel number, as also demonstrated in our work.

Vessels are long, continuous tubes formed by the fusion of multiple vessel elements and constitute the main conductive cells of the xylem in most angiosperms (Aloni, 2013; Evert, 2013). In stems, elevated auxin concentrations are generally associated with a greater number of vessels with larger diameters, whereas lower concentrations tend to produce fewer, narrower, and more lignified vessels (Bhalerao and Fischer, 2017). Our results in cherry tomato and wheat partially align with these observations. Both LNP–IAA treatments increased vessel number, with the 100 μg mL^{-1} concentration showing the strongest effect in tomato. In wheat, LNP–IAA at 0.05 μg mL^{-1} exhibited greatest effect, along with the 100 μg mL^{-1} free IAA treatment.

A similar pattern was observed for vessel element diameter, particularly in wheat. The modulation of vessel diameter by IAA concentration is closely associated with the timing of maturation and differentiation of conductive cells (Buttò et al., 2019). In addition, turgor pressure and cell wall extensibility are key determinants of vessel size, with IAA and ABA acting as major regulatory signals in this process (Ren et al., 2025). High auxin concentrations promote rapid differentiation, whereas lower concentrations allow slower cell maturation and greater deposition of cellulose and lignin in the secondary wall, an important feature that enhances resistance to abiotic stress and reduces the risk of xylem cavitation (Barros et al., 2015; Cao et al., 2020; Moulin et al., 2022).

Although treatments with free and encapsulated IAA reached similar final values toward the end of the evaluation period, temporal modeling revealed distinct dynamics in their effects that varied between species. In cherry tomato, both LNP–IAA treatments at 0.05 and 100 μg mL^{-1} promoted significant daily growth rates (4.4 % and 4.2 % per day, respectively), followed by free IAA at the same concentrations (1.7 % and –0.5 % per day) relative to the control. Interestingly, empty nanoparticles also produced a daily growth effect (3.1 % per day), exceeding that of free IAA applications. In wheat, both 100 μg mL^{-1} treatments resulted in a significant daily increase in vascular cylinder size, averaging approximately 3.5 % per day. In contrast, the 0.05 μg mL^{-1} treatments, although showing slightly higher daily rates (1.7 % per day), were not statistically significant. Additionally, treatment with unloaded LNPs did not promote daily expansion of the vascular cylinder. These results raise important considerations regarding the distinct activity patterns of lignin nanoparticles.

The higher initial daily growth rate observed for LNP treatments suggests that nanoencapsulation provides an early temporal advantage, promoting faster expansion shortly after application—likely due to the gradual release of the hormone and its increased bioavailability in target tissues. This behavior underscores the benefits of nanoencapsulation for various bioactive compounds, demonstrating that this process not only preserves hormone efficacy but also enhances their sustained activity over time (do Espirito Santo Pereira et al., 2021; Duhan et al., 2017; Fraceto et al., 2016).

This advantage is further supported by the 100 μg mL^{-1} concentration in cherry tomato, where treatment with free IAA resulted in a negative daily growth rate, indicating possible phytotoxicity or inhibition of cell expansion at high auxin levels. In contrast, LNP–IAA at the same concentration did not exhibit this effect, maintaining a growth pattern comparable to lower concentrations. This difference highlights the capacity of nanoencapsulation to provide controlled hormone release, preventing toxic peaks while sustaining physiological activity (Mondéjar-López et al., 2024; Paramo et al., 2020). Over time, however, the treatments tended to converge, suggesting that physiological constraints (such as hormonal response saturation, anatomical limitations, and the duration of the experimental period) may modulate growth at later developmental stages.

Furthermore, our results revealed that the application of unloaded LNPs exerted a clear biological effect, even though multivariate analyses indicated a negative correlation with the measured variables. This apparent paradox can be explained by two main hypotheses. First, the presence of nanoparticles, regardless of their bioactive load, may induce mild oxidative stress in plant tissues, activating genetic responses that reorganize growth patterns and modulate gene expression (Hossain et al., 2015; Munir et al., 2023). Second, the physicochemical properties of the nanoparticles themselves, such as composition, size, and surface charge, may directly interact with cellular components, triggering alternative signaling pathways that influence plant development (Zhang et al., 2023). In the case of LNPs, the chemical structure of lignin, with its phenolic groups and redox-active properties, can activate signaling cascades that modulate growth independently of hormonal stimuli, as previously documented for lignin nanoparticles in maize (Del Buono et al., 2021).

Additionally, carvacrol, the surfactant used in the LNP formulation, may also contribute to the observed biological responses (Faleiro et al., 2025). This essential oil has attracted increasing attention in agriculture due to its antifungal and antibacterial properties (Friedman, 2014; Marchese et al., 2018). However, it can also exhibit phytotoxic effects even at low concentrations, inhibiting the growth of several weed species (Chaimovitsh et al., 2017; de Assis Alves et al., 2018; Hazrati et al., 2017; Kordali et al., 2008). Therefore, its presence in the formulation may partly account for the intrinsic biological activity of the LNP treatments. The overall influence of this compound on LNP performance remains uncertain, and future studies specifically designed to isolate and evaluate the activity of carvacrol will be essential to fully elucidate its role in modulating nanoparticle behavior.

Finally, our results highlight contrasting responses between cherry tomato and wheat to LNP–IAA treatments, reflecting their anatomical and physiological differences. Cherry tomato (a eudicot) exhibited greater sensitivity to high concentrations, showing negative effects likely associated with the saturation of hormone transport systems within its continuous vascular cylinder. In contrast, wheat (a monocot) responded positively to the same concentrations, suggesting that its vascular system —organized in discrete, independent bundles — confers greater resilience to hormonal fluctuations or requires higher concentrations to trigger direct physiological responses. Plant responses to exogenous growth regulators vary widely among species, as differences in distribution and transport pathways across plant groups ultimately influence both the intensity and spatial pattern of the physiological response (Anfang and Shani, 2021; Blázquez et al., 2020; Rademacher, 2015).

These findings contribute significantly to ongoing discussions in the literature concerning how plant morphology influences nanoparticle behavior and response (Zhang et al., 2023). They emphasize the need for species-specific evaluation frameworks that account for unique anatomical adaptations and physiological specializations when assessing nanocarrier efficacy and optimal concentration. Our results

underscore that generalized nanoparticle application protocols may be suboptimal, as absorption efficiency and systemic effects are fundamentally governed by the morphological and functional traits inherent to each species.

Although our study demonstrates the potential of polymeric nanoparticles and the advantages of nanoencapsulating plant growth regulators, several questions remain unresolved, particularly concerning nanoparticle behavior and the resulting physiological responses. The literature still lacks systematic investigations evaluating the impact of nanoencapsulated growth regulators on vascular development in plants, which limits broader comparative analyses. Moreover, while the role and mechanisms of auxin action are well established in Arabidopsis, information on auxin dynamics in other species (especially monocots), which possess distinct anatomical and physiological characteristics remains scarce. These knowledge gaps highlight the need for more comprehensive studies examining the effects of nanoencapsulation across diverse plant systems, considering differences in vascular architecture, hormonal sensitivity, and secondary metabolism. Such investigations will be essential for optimizing agricultural applications and promote the safe and effective use of this technology in economically important crops.

5. Conclusion

This study demonstrates that lignin nanoparticles encapsulating indole-3-acetic acid (LNP–IAA) effectively modulate xylem development in both cherry tomato and wheat, providing controlled hormonal action without inducing phytotoxic effects. Nanoencapsulation preserved the bioactivity of IAA while enabling gradual release and enhanced physiological performance relative to free hormone applications. The contrasting optimal concentrations between species — 0.05 μg mL^{-1} for cherry tomato and 100 μg mL^{-1} for wheat — highlight how vascular architecture fundamentally determines nanocarrier efficiency. Additionally, unloaded LNPs exhibited intrinsic biological activity, revealing growth-modulating properties independent of hormone loading. Together, these findings position LNPs as a sustainable and versatile nanoplatform for the targeted delivery of plant growth regulators, offering new opportunities for precise control of vascular development and productivity in crops.

Declaration of Competing Interest

Given their role as **Plant Nano Biology**, **Rodrigo Faleiro** was not involved in the peer-review of this article and has no access to information regarding its peer-review. Full responsibility for the editorial process for this article was delegated to another journal editor.

CRediT authorship contribution statement

Marcelo Rodrigo Pace: Writing – review & editing, Writing – original draft, Data curation. **Magda Andréia Tessmer:** Writing – review & editing, Writing – original draft, Validation, Supervision. **Rodrigo Faleiro:** Writing – review & editing, Writing – original draft, Methodology, Investigation, Funding acquisition, Formal analysis, Data curation, Conceptualization. **Juliana Lischka Sampaio Mayer:** Writing – review & editing, Writing – original draft, Validation, Methodology, Investigation, Funding acquisition, Conceptualization. **Anderson do Espirito Santo Pereira:** Writing – review & editing, Writing – original draft, Methodology, Formal analysis. **Leonardo Fernandes Fraceto:** Writing – review & editing, Writing – original draft, Project administration, Methodology.

Funding

These works are funded by the São Paulo Research Foundation (FAPESP), the National Council for Scientific and Technological Development (CNPq) and Coordenação de Aperfeiçoamento de Pessoal de Nível Superior (Capes) – Brazil.

Declaration of Competing interest

The authors declare no competing interests.

Acknowledgements

Rodrigo Faleiro thanks the São Paulo State Research Support Foundation (FAPESP) for a doctorate scholarship (2022/02559–4). Marcelo R. Pace thanks DGAPA PAPIIT (IN204025) and SECIHTI Frontiers (CF-2023-I-255). Leonardo F. Fraceto thanks the São Paulo State Research Support Foundation (FAPESP, grants CBioClima — #2021/10639–5 and #2017/21004–5), the Brazilian National Council for Scientific and Technological Development (CNPq-MCTI-INCT NanoAgro #405924/2022–4, #308439/2021–0) and the Coordenação de Aperfeiçoamento de Pessoal de Nível Superior – Brasil (CAPES - MEC INCTNa- noAgro #88887.953443/2024–00). Juliana Mayer thanks CNPq (productivity grant 309175/2023–2).

Appendix A. Supporting information

Supplementary data associated with this article can be found in the online version at doi:10.1016/j.plana.2025.100226.

Data Availability

Data will be made available on request.

References

Aichinger, E., Kornet, N., Friedrich, T., Laux, T., 2012. Plant stem cell niches. Annu Rev. Plant Biol. 63, 615–636. https://doi.org/10.1146/annurev-arplant-042811-105555.

Aloni, R., 2013. Role of hormones in controlling vascular differentiation and the mechanism of lateral root initiation. Planta 238, 819–830. https://doi.org/10.1007/s00425-013-1927-8.

Anfang, M., Shani, E., 2021. Transport mechanisms of plant hormones. Curr. Opin. Plant Biol. 63, 102055. https://doi.org/10.1016/j.pbi.2021.102055.

de Assis Alves, T., Fontes Pinheiro, P., Miranda Praça-Fontes, M., Fonseca Andrade-Vieira, L., Barelo Corrêa, K., de Assis Alves, T., da Cruz, F.A., Lacerda Júnior, V., Ferreira, A., Bastos Soares, T.C., 2018. Toxicity of thymol, carvacrol and their respective phenoxyacetic acids in Lactuca sativa and Sorghum bicolor. Ind. Crops Prod. 114, 59–67. https://doi.org/10.1016/j.indcrop.2018.01.071.

Athanassiou, C.G., Kavallieratos, N.G., Benelli, G., Losic, D., Usha Rani, P., Desneux, N., 2018. Nanoparticles for pest control: current status and future perspectives. J. Pest Sci. 91 (2004), 1–15. https://doi.org/10.1007/s10340-017-0898-0.

Auffan, M., Rose, J., Bottero, J.-Y., Lowry, G.V., Jolivet, J.-P., Wiesner, M.R., 2009. Towards a definition of inorganic nanoparticles from an environmental, health and safety perspective. Nat. Nanotechnol. 4, 634–641. https://doi.org/10.1038/nnano.2009.242.

Avellan, A., Yun, J., Morais, B.P., Clement, E.T., Rodrigues, S.M., Lowry, G.V., 2021. Critical review: role of inorganic nanoparticle properties on their foliar uptake and *in Planta* Translocation. Environ. Sci. Technol. 55, 13417–13431. https://doi.org/10.1021/acs.est.1c00178.

Azim, Z., Singh, N.B., Singh, A., Amist, N., Niharika, Khare, S., Yadav, R.K., Bano, C., Yadav, V., 2023. A review summarizing uptake, translocation and accumulation of nanoparticles within the plants: current status and future prospectus. J. Plant Biochem Biotechnol. 32, 211–224. https://doi.org/10.1007/s13562-022-00800-6.

Barros, J., Serk, H., Granlund, I., Pesquet, E., 2015. The cell biology of lignification in higher plants. Ann. Bot. 115, 1053–1074. https://doi.org/10.1093/aob/mcv046.

Beach, M.A., Nayanathara, U., Gao, Y., Zhang, C., Xiong, Y., Wang, Y., Such, G.K., 2024. Polymeric Nanoparticles for Drug Delivery. Chem. Rev. 124, 5505–5616. https://doi.org/10.1021/acs.chemrev.3c00705.

Bhalerao, R.P., Fischer, U., 2017. Environmental and hormonal control of cambial stem cell dynamics. J. Exp. Bot. 68, 79–87. https://doi.org/10.1093/jxb/erw466.

Björklund, S., Antti, H., Uddestrand, I., Moritz, T., Sundberg, B., 2007. Cross-talk between gibberellin and auxin in development of Populus wood: gibberellin stimulates polar auxin transport and has a common transcriptome with auxin. Plant J. 52, 499–511. https://doi.org/10.1111/j.1365-313X.2007.03250.x.

Blázquez, M.A., Nelson, D.C., Weijers, D., 2020. Evolution of Plant Hormone Response Pathways. Annu Rev. Plant Biol. 71, 327–353. https://doi.org/10.1146/annurev-arplant-050718-100309.

Buttò, V., Rossi, S., Deslauriers, A., Morin, H., 2019. Is size an issue of time? Relationship between the duration of xylem development and cell traits. Ann. Bot. 123, 1257–1265. https://doi.org/10.1093/aob/mcz032.

Cabello, J.V., Chan, R.L., 2019. Arabidopsis and sunflower plants with increased xylem area show enhanced seed yield. Plant J. 99, 717–732. https://doi.org/10.1111/tpj.14356.

Campos, E.V.R., do Espirito Santo Pereira, A., de Oliveira, J.L., Villarreal, G.P.U., Fraceto, L.F., 2022. Nature-Based Nanocarrier System: An Eco-friendly Alternative for Improving Crop Resilience to Climate Changes. Anthr. Sci. 1, 396–403. https://doi.org/10.1007/s44177-022-00029-x.

Cao, S., Huang, C., Luo, L., Zheng, S., Zhong, Y., Sun, J., Gui, J., Li, L., 2020. Cell-Specific Suppression of 4-Coumarate-CoA Ligase Gene Reveals Differential Effect of Lignin on Cell Physiological Function in Populus. Front Plant Sci. 11. https://doi.org/10.3389/fpls.2020.589729.

Chaimovitsh, D., Shachter, A., Abu-Abied, M., Rubin, B., Sadot, E., Dudai, N., 2017. Herbicidal Activity of Monoterpenes Is Associated with Disruption of Microtubule Functionality and Membrane Integrity. Weed Sci. 65, 19–30. https://doi.org/10.1614/WS-D-16-00044.1.

Chauhan, P.S., 2020. Lignin nanoparticles: Eco-friendly and versatile tool for new era. Bioresour. Technol. Rep. 9, 100374. https://doi.org/10.1016/j.biteb.2019.100374.

Cifuentes, Z., Custardoy, L., de la Fuente, J.M., Marquina, C., Ibarra, M.R., Rubiales, D., Pérez-de-Luque, A., 2010. Absorption and translocation to the aerial part of magnetic carbon-coated nanoparticles through the root of different crop plants. J. Nanobiotechnology 8, 26. https://doi.org/10.1186/1477-3155-8-26.

Del Buono, D., Luzi, F., Puglia, D., 2021. Lignin Nanoparticles: A promising tool to improve Maize physiological, biochemical, and Chemical Traits. Nanomaterials 11, 846. https://doi.org/10.3390/nano11040846.

Dubey, S., Nair, R., Jain, S., Sharma, A., Thakur, H., Koushale, M., Ahirwar, S., 2024. Effect of Foliar-applied Plant Growth Regulators on Coriander (Coriandrum sativum L.) to Regulate Growth and Yield Attributes. Arch. Curr. Res. Int. 24, 217–226. https://doi.org/10.9734/acri/2024/v24i9886.

Duhan, J.S., Kumar, R., Kumar, N., Kaur, P., Nehra, K., Duhan, S., 2017. Nanotechnology: The new perspective in precision agriculture. Biotechnol. Rep. 15, 11–23. https://doi.org/10.1016/j.btre.2017.03.002.

do Espirito Santo Pereira, A., Caixeta Oliveira, H., Fernandes Fraceto, L., Santaella, C., 2021. Nanotechnology potential in seed priming for sustainable agriculture. Nanomaterials 11, 267. https://doi.org/10.3390/nano11020267.

Eswaran, G., Zhang, X., Rutten, J.P., Han, J., Iida, H., López Ortiz, J., Mäkilä, R., Wybouw, B., Planterose Jiménez, B., Vainio, L., Porcher, A., Leal Gavarron, M., Zhang, J., Blomster, T., Wang, X., Dolan, D., Smetana, O., Brady, S.M., Kucukoglu Topcu, M., ten Tusscher, K., Etchells, J.P., Mähönen, A.P., 2024. Identification of cambium stem cell factors and their positioning mechanism. Science 386 (1979), 646–653. https://doi.org/10.1126/science.adj8752.

Evert, R.F., 2013. Esau's plant anatomy: meristems, cells and tissues of the plant body: their structure, function and development., 3o ed. ed. Blucher, São Paulo.

Faleiro, R., Tessmer, M.A., Santo Pereira, A.E., Fraceto, L.F., Rampasso, M.S., Miranda, M.T., Pissolato, M.D., Cassola, F., Ribeiro, R.V., Mayer, J.L.S., 2025. Assessment of the impact of biodegradable lignin nanoparticles encapsulating IAA on tomato development: from seed to fruit. BMC Plant Biol. 25, 768. https://doi.org/10.1186/s12870-025-06539-1.

Falsini, S., Clemente, I., Papini, A., Tani, C., Schiff, S., Salvatici, M.C., Petruccelli, R., Benelli, C., Giordano, C., Gonnelli, C., Ristori, S., 2019. When Sustainable Nanochemistry Meets Agriculture: Lignin Nanocapsules for Bioactive Compound Delivery to Plantlets. ACS Sustain Chem. Eng. 7, 19935–19942. https://doi.org/10.1021/acssuschemeng.9b05462.

Falsini, S., Tani, C., Schiff, S., Gonnelli, C., Clemente, I., Ristori, S., Papini, A., 2020. A new method for the direct tracking of in vivo lignin nanocapsules in Eragrostis tef (Poaceae) tissues. Eur. J. Histochem. 64. https://doi.org/10.4081/ejh.2020.3112.

Fraceto, L.F., Grillo, R., de Medeiros, G.A., Scognamiglio, V., Rea, G., Bartolucci, C., 2016. Nanotechnology in agriculture: Which innovation potential does it have? Front Environ. Sci. 4. https://doi.org/10.3389/fenvs.2016.00020.

Friedman, M., 2014. Chemistry and Multibeneficial Bioactivities of Carvacrol (4-Isopropyl-2-methylphenol), a Component of Essential Oils Produced by Aromatic Plants and Spices. J. Agric. Food Chem. 62, 7652–7670. https://doi.org/10.1021/jf5023862.

Hacke, U., 2001. Functional and ecological Xylem anatomy. Funct. Ecol. Xylem Anat. 4, 1–281. https://doi.org/10.1007/978-3-319-15783-2.

Hazrati, H., Saharkhiz, M.J., Niakousari, M., Moein, M., 2017. Natural herbicide activity of Satureja hortensis L. essential oil nanoemulsion on the seed germination and morphophysiological features of two important weed species. Ecotoxicol. Environ. Saf. 142, 423–430. https://doi.org/10.1016/j.ecoenv.2017.04.041.

Hossain, Z., Mustafa, G., Komatsu, S., 2015. Plant Responses to Nanoparticle Stress. Int J. Mol. Sci. 16, 26644–26653. https://doi.org/10.3390/ijms161125980.

Janmohammadi, M., Sabaghnia, N., 2023. Effects of foliar spray of nano-micronutrient and growth regulators on safflower (Carthamus tinctorius L.) performance. Plant Nano Biol. 5, 100045. https://doi.org/10.1016/j.plana.2023.100045.

Johnsson, C., Jin, X., Xue, W., Dubreuil, C., Lezhneva, L., Fischer, U., 2019. The plant hormone auxin directs timing of xylem development by inhibition of secondary cell wall deposition through repression of secondary wall NAC-domain transcription factors. Physiol. Plant 165, 673–689. https://doi.org/10.1111/ppl.12766.

Kordali, S., Cakir, A., Ozer, H., Cakmakci, R., Kesdek, M., Mete, E., 2008. Antifungal, phytotoxic and insecticidal properties of essential oil isolated from Turkish Origanum acutidens and its three components, carvacrol, thymol and p-cymene. Bioresour. Technol. 99, 8788–8795. https://doi.org/10.1016/j.biortech.2008.04.048.

Korpayev, S., Karakeçili, A., Dumanoğlu, H., Ibrahim Ahmed Osman, S., 2021. Chitosan and silver nanoparticles are attractive auxin carriers: A comparative study on the adventitious rooting of microcuttings in apple rootstocks. Biotechnol. J. 16, 2100046. https://doi.org/10.1002/biot.202100046.

Low, L.E., Teh, K.C., Siva, S.P., Chew, I.M.L., Mwangi, W.W., Chew, C.L., Goh, B.-H., Chan, E.S., Tey, B.T., 2021. Lignin nanoparticles: The next green nanoreinforcer with wide opportunity. Environ. Nanotechnol. Monit. Manag 15, 100398. https://doi.org/10.1016/j.enmm.2020.100398.

Marchese, A., Arciola, C.R., Coppo, E., Barbieri, R., Barreca, D., Chebaibi, S., Sobarzo-Sánchez, E., Nabavi, S.F., Nabavi, S.M., Daglia, M., 2018. The natural plant compound carvacrol as an antimicrobial and anti-biofilm agent: mechanisms, synergies and bio-inspired anti-infective materials. Biofouling 34, 630–656. https://doi.org/10.1080/08927014.2018.1480756.

Maruyama, C.R., Guilger, M., Pascoli, M., Bileshy-José, N., Abhilash, P.C., Fraceto, L.F., de Lima, R., 2016. Nanoparticles based on chitosan as carriers for the combined herbicides imazapic and imazapyr. Sci. Rep. 6, 19768. https://doi.org/10.1038/srep19768.

Milhinhos, A., Miguel, C.M., 2013. Hormone interactions in xylem development: a matter of signals. Plant Cell Rep. 32, 867–883. https://doi.org/10.1007/s00299-013-1420-7.

Mondéjar-López, M., García-Simarro, M.P., Navarro-Simarro, P., Gómez-Gómez, L., Ahrazem, O., Niza, E., 2024. A review on the encapsulation of "eco-friendly" compounds in natural polymer-based nanoparticles as next generation nano-agrochemicals for sustainable agriculture and crop management. Int J. Biol. Macromol. 280, 136030. https://doi.org/10.1016/j.ijbiomac.2024.136030.

Moreno-Piovano, G.S., Moreno, J.E., Cabello, J.V., Arce, A.L., Otegui, M.E., Chan, R.L., 2017. A role for LAX2 in regulating xylem development and lateral-vein symmetry in the leaf. Ann. Bot. 120, 577–590. https://doi.org/10.1093/aob/mcx091.

Moulin, J.C., de Souza Ribeiro, D., Vidaurre, G.B., Braga Mulin, L., Moreira, S.I., 2022. Effect of drought stress on the formation and lignification of eucalyptus wood cells. IAWA J. 43, 263–275. https://doi.org/10.1163/22941932-bja10092.

Munir, N., Gulzar, W., Abideen, Z., Hasanuzzaman, M., El-Keblawy, A., Zhao, F., 2023. Plant–Nanoparticle Interactions: Transcriptomic and Proteomic Insights. Agronomy 13, 2112. https://doi.org/10.3390/agronomy13082112.

NDABA, B., ROOPNARAIN, A., RAMA, H., MAAZA, M., 2022. Biosynthesized metallic nanoparticles as fertilizers: An emerging precision agriculture strategy. J. Integr. Agric. 21, 1225–1242. https://doi.org/10.1016/S2095-3119(21)63751-6.

Onyenedum, J.G., Pace, M.R., 2021. The role of ontogeny in wood diversity and evolution. Am. J. Bot. 108, 2331–2355. https://doi.org/10.1002/ajb2.1801.

Paramo, L.A., Feregrino-Pérez, A.A., Guevara, R., Mendoza, S., Esquivel, K., 2020. Nanoparticles in agroindustry: applications, toxicity, challenges, and trends. Nanomaterials 10, 1654. https://doi.org/10.3390/nano10091654.

Paque, S., Weijers, D., 2016. Auxin: the plant molecule that influences almost anything. BMC Biol. 14, 67. https://doi.org/10.1186/s12915-016-0291-0.

Pereira, A., do, E.S., Oliveira, H.C., Fraceto, L.F., 2019. Polymeric nanoparticles as an alternative for application of gibberellic acid in sustainable agriculture: a field study. Sci. Rep. 9, 7135. https://doi.org/10.1038/s41598-019-43494-y.

Pereira, A., do, E.S., Luiz de Oliveira, J., Maira Savassa, S., Barbara Rogério, C., Araujo de Medeiros, G., Fraceto, L.F., 2022. Lignin nanoparticles: New insights for a sustainable agriculture. J. Clean. Prod. 345, 131145. https://doi.org/10.1016/j.jclepro.2022.131145.

Pereira, A.E.S., Silva, P.M., Oliveira, J.L., Oliveira, H.C., Fraceto, L.F., 2017. Chitosan nanoparticles as carrier systems for the plant growth hormone gibberellic acid. Colloids Surf. B Biointerfaces 150, 141–152. https://doi.org/10.1016/j.colsurfb.2016.11.027.

Pham, T.P.T., Le, V.H., Le, T.T., Trinh, V.B., 2023. Effects of different plant growth regulators as the foliar application on growth and flower quality of potted rose (Rosa chinensis Jacq. cv. Nhung). CTU J. Innov. Sustain. Dev. 15, 45–50. https://doi.org/10.22144/ctu.jen.2023.019.

Pizzolato, T.D., Sundberg, M.D., 2001. Initiation of the vascular system in the shoot of zea mays l. (poaceae). i. the procambial nodal plexus. Int J. Plant Sci. 162, 539–566. https://doi.org/10.1086/320143.

Preisler, A.C., Guariz, H.R., Carvalho, L.B., Pereira, A., do, E.S., de Oliveira, J.L., Fraceto, L.F., Dalazen, G., Oliveira, H.C., 2022. Phytotoxicity evaluation of poly (ε-caprolactone) nanocapsules prepared using different methods and compositions in Brassica juncea seeds. Plant Nano Biol. 1, 100003. https://doi.org/10.1016/j.plana.2022.100003.

Quintela, A.L., Santos, M.F.C., de Lima, R.F., Mayer, J.L.S., Marcheafave, G.G., Arruda, M.A.Z., Tormena, C.F., 2024. Influence of Silver Nanoparticles on the Metabolites of Two Transgenic Soybean Varieties: An NMR-Based Metabolomics Approach. J. Agric. Food Chem. 72, 12281–12294. https://doi.org/10.1021/acs.jafc.4c00756.

Rademacher, W., 2015. Plant Growth Regulators: Backgrounds and uses in plant production. J. Plant Growth Regul. 34, 845–872. https://doi.org/10.1007/s00344-015-9541-6.

Rani, S., Kumari, N., Sharma, V., 2023. Uptake, translocation, transformation and physiological effects of nanoparticles in plants. Arch. Agron. Soil Sci. 69, 1579–1599. https://doi.org/10.1080/03650340.2022.2103549.

Ren, A., Yang, Y., Huang, Y., Wan, Y., Liu, Y., 2025. ExogenouS Auxin Enhances Stem Straightness In Paeonia Lactiflora Cultivar By Modulating Cellulose Development And Vascular Tissue. J. Plant Growth Regul. 44, 660–673. https://doi.org/10.1007/s00344-024-11471-z.

Růžička, K., Ursache, R., Hejátko, J., Helariutta, Y., 2015. Xylem development – from the cradle to the grave. N. Phytol. 207, 519–535. https://doi.org/10.1111/nph.13383.

Sanchez, P., Nehlin, L., Greb, T., 2012. From thin to thick: major transitions during stem development. Trends Plant Sci. 17, 113–121. https://doi.org/10.1016/j.tplants.2011.11.004.

Scholz, A., Klepsch, M., Karimi, Z., Jansen, S., 2013. How to quantify conduits in wood? Front Plant Sci. 4. https://doi.org/10.3389/fpls.2013.00056.

Shahsavar, A.R., Farkhondeh, H., Sayyad-Amin, P., 2024. The effect of foliar spraying of naphthalene acetic acid, gibberellic acid, kinetin, putrescine and salicylic acid on physicochemical properties of 'Shahabi' date fruit. Sci. Rep. 14, 31360. https://doi.org/10.1038/s41598-024-82657-4.

Simon, S., Skůpa, P., Viaene, T., Zwiewka, M., Tejos, R., Klíma, P., Čarná, M., Rolčík, J., De Rycke, R., Moreno, I., Dobrev, P.I., Orellana, A., Zažímalová, E., Friml, J., 2016. PIN6 auxin transporter at endoplasmic reticulum and plasma membrane mediates auxin homeostasis and organogenesis in Arabidopsis. New Phytol. 211, 65–74. https://doi.org/10.1111/nph.14019.

Spielman-Sun, E., Avellan, A., Bland, G.D., Tappero, R.V., Acerbo, A.S., Unrine, J.M., Giraldo, J.P., Lowry, G.V., 2019. Nanoparticle surface charge influences translocation and leaf distribution in vascular plants with contrasting anatomy. Environ. Sci.: Nano 6, 2508–2519. https://doi.org/10.1039/C9EN00626E.

Sun, D., Hussain, H.I., Yi, Z., Siegele, R., Cresswell, T., Kong, L., Cahill, D.M., 2014. Uptake and cellular distribution, in four plant species, of fluorescently labeled mesoporous silica nanoparticles. Plant Cell Rep. 33, 1389–1402. https://doi.org/10.1007/s00299-014-1624-5.

Wang, D., Saleh, N.B., Byro, A., Zepp, R., Sahle-Demessie, E., Luxton, T.P., Ho, K.T., Burgess, R.M., Flury, M., White, J.C., Su, C., 2022. Nano-enabled pesticides for sustainable agriculture and global food security. Nat. Nanotechnol. 17, 347–360. https://doi.org/10.1038/s41565-022-01082-8.

Wang, X., Xie, H., Wang, P., Yin, H., 2023. Nanoparticles in Plants: Uptake, Transport and Physiological Activity in Leaf and Root. Materials 16, 3097. https://doi.org/10.3390/ma16083097.

Xu, C., Shen, Y., He, F., Fu, X., Yu, H., Lu, W., Li, Y., Li, C., Fan, D., Wang, H.C., Luo, K., 2019. Auxin-mediated Aux/ <scp>IAA</scp> - <scp>ARF</scp> - <scp>HB</scp> signaling cascade regulates secondary xylem development in Populus. N. Phytol. 222, 752–767. https://doi.org/10.1111/nph.15658.

Xu, T., Wang, D., Si, Y., Kong, Y., Shao, X., Geng, Y., Lv, Y., Wang, Y., 2024. Plant Growth Regulators Enhance Maize (Zea mays L.) Yield under High Density by Optimizing Canopy Structure and Delaying Leaf Senescence. Agronomy 14, 1262. https://doi.org/10.3390/agronomy14061262.

Yan, A., Chen, Z., 2019. Impacts of silver nanoparticles on plants: a focus on the phytotoxicity and underlying mechanism. Int J. Mol. Sci. 20, 1003. https://doi.org/10.3390/ijms20051003.

Yang, L., Zhu, S., 2022. The interconnected relationship between auxin concentration gradient changes in chinese fir radial stems and dynamic cambial activity. Forests 13, 1698. https://doi.org/10.3390/f13101698.

Ye, Z.-H., 2002. V <scp>ASCULAR</scp> T <scp>ISSUE</scp> D <scp>IFFERENTIATION AND</scp> P <scp>ATTERN</scp> F <scp>ORMATION IN</scp> P <scp>LANTS</scp>. Annu Rev. Plant Biol. 53, 183–202. https://doi.org/10.1146/annurev.arplant.53.100301.135245.

Zhang, Y., Martinez, M.R., Sun, H., Sun, M., Yin, R., Yan, J., Marelli, B., Giraldo, J.P., Matyjaszewski, K., Tilton, R.D., Lowry, G.V., 2023. Charge, Aspect Ratio, and Plant Species Affect Uptake Efficiency and Translocation of Polymeric Agrochemical Nanocarriers. Environ. Sci. Technol. 57, 8269–8279. https://doi.org/10.1021/acs.est.3c01154.

Zhu, J., Li, J., Shen, Y., Liu, S., Zeng, N., Zhan, X., White, J.C., Gardea-Torresdey, J., Xing, B., 2020. Mechanism of zinc oxide nanoparticle entry into wheat seedling leaves. Environ. Sci. Nano 7, 3901–3913. https://doi.org/10.1039/D0EN00658K.

Zhu, J., Wang, J., Zhan, X., Li, A., White, J.C., Gardea-Torresdey, J.L., Xing, B., 2021. Role of charge and size in the translocation and distribution of zinc oxide particles in wheat cells. ACS Sustain Chem. Eng. 9, 11556–11564. https://doi.org/10.1021/acssuschemeng.1c04080.